Molecular Pharmacology Fast Forward. Published on December 23, 2013 as doi: 10.1124/mol.113.088526

Pore exposed tyrosine residues of P-glycoprotein are important hydrogen bonding partners for drugs

Yaprak Dönmez Cakil, Narakorn Khunweeraphong, Zahida Parveen, Diethart Schmid, Matthias Artaker, Gerhard F. Ecker, Harald H. Sitte, Oliver Pusch, Thomas Stockner, Peter Chiba

Institute of Medical Chemistry, Medical University of Vienna, Waehringerstrasse 10, 1090 Vienna, Austria (Y.D.C., N.K., Z.P., P.C.)

Department of Biochemistry, Abdul Wali Khan University Mardan, Pakistan (Z.P.)

Institute of Pharmacology, Medical University of Vienna, Waehringerstrasse 13A, 1090 Vienna, Austria (Y.D.C., T.S., H.H.S.)

Institute of Physiology, Medical University of Vienna, Schwarzspanierstrasse 17, 1090 Vienna, Austria (D.S.)

Department of Medical Biochemistry, Max F. Perutz Laboratories, Medical University of Vienna, Dr. Bohrgasse 9, 1030 Vienna, Austria (M.A.)

Emerging Field Pharmacoinformatics, Dept. of Medicinal Chemistry, University of Vienna, Althanstrasse 14, 1090 Vienna, Austria (G.F.E.)

Department of Cell and Developmental Biology, Medical University of Vienna, Schwarzspanierstraße 17, 1090 Vienna, Austria (O.P.)

Molecular Pharmacology Fast Forward. Published on December 23, 2013 as DOI: 10.1124/mol.113.088526
This article has not been copyedited and formatted. The final version may differ from this version.

Running title page

Pore exposed ABCB1 tyrosines form hydrogen bonds with drugs

Address correspondence to:

Thomas Stockner, Institute of Pharmacology, Waehringerstrasse 13A, 1090 Vienna, Austria, phone +43 1 40160 31361, Fax: +43 1 40160 931300, email: thomas.stockner@meduniwien.ac.at

Number of text pages: 27

Number of tables: 0

Number of figures: 5

Number of references: 33

Number of words in

Abstract: 142

Introduction: 441

Discussion: 1437

d) List of non-standard abbreviations

ABC, ATP-binding cassette; P-gp, P-glycoprotein; MDR, multidrug resistance; TMD, transmembrane domain; NBD, nucleotide binding domain; rh123, rhodamine123;

Molecular Pharmacology Fast Forward. Published on December 23, 2013 as DOI: 10.1124/mol.113.088526
This article has not been copyedited and formatted. The final version may differ from this version.

Abstract

The multispecific efflux transporter P-glycoprotein plays an important role in drug disposition. Substrate translocation occurs along the interface of its transmembrane domains. The rotational C2 symmetry of ABC-transporters implies the existence of two symmetry related sets of substrate-interacting amino acids. These sets are identical in homodimeric transporters, and remain evolutionarily related in full transporters such as P-glycoprotein, where substrates bind preferentially, but non-exclusively to one of two binding sites. We explored the role of pore exposed tyrosines for hydrogen-bonding interactions with propafenone type ligands in their preferred binding site 2. Tyrosine 953 is shown to form hydrogen-bonds with propafenone analogs, but also with the preferred site 1 substrate rhodamine123. Furthermore, an accessory role of tyrosine 950 for binding of selected propafenone analogs is demonstrated. The present study demonstrates the importance of domain interface tyrosine residues for interaction of small molecules with P-glycoprotein.

Molecular Pharmacology Fast Forward. Published on December 23, 2013 as DOI: 10.1124/mol.113.088526
This article has not been copyedited and formatted. The final version may differ from this version.

Introduction

ATP-binding cassette (ABC) proteins form one of the largest families of transmembrane proteins. The human genome contains 48 genes encoding for ABC proteins, the majority of which are transporters. Mutations in at least 17 ABC transporters have been linked to disease etiologies (Linton et al., 2011). The minimal functional unit of a transporter consists of four domains: two transmembrane domains (TMDs), which form the solute conduits and two nucleotide binding domains (NBDs), which provide the energy for solute translocation by ATP binding and hydrolysis. Human P-glycoprotein (P-gp, ABCB1) is a multidrug resistance transporter, which plays a central role in drug disposition. Therefore, early profiling of developmental compounds includes routine screening for P-gp substrate properties (Giacomini et al., 2010).

A mechanistic model for cargo transport of ABC efflux transporters remains elusive, despite a large body of biochemical evidence. The present study characterizes the contribution of hydrogen bonding interactions between propafenone type ligands and selected pore exposed tyrosine OH-groups. Propafenones have been characterized extensively in previous QSAR studies and demonstrated to be both substrates and inhibitors of P-glycoprotein (Schmid et al., 1999). Tyrosine residues are known to play a pivotal role for molecular recognition in biological systems, including domain interface and active site interactions. Tyrosines are amphipathic residues, capable of forming hydrophobic, hydrogen-bonding, π-π and π-cation interactions. They were shown to make a large contribution to protein stability (Pace et al., 2001), but nevertheless contribute to structural plasticity of binding regions (Mian et al., 1991). The rigidity of the aromatic ring is associated with a reduced loss of conformational entropy upon immobilization in binding interfaces (Koide and Sidhu, 2009). The amphipathic nature of tyrosines allows them to readily tolerate changes in the polarity of their environment (MacCallum et al., 2007). Molecular dynamics simulations suggest that rotamers adopt different positions in the drug binding pocket that allow them to contribute to poly-specificity (Liu et al., 2013). The known requirement for hydrogen bonding interaction of

Molecular Pharmacology Fast Forward. Published on December 23, 2013 as DOI: 10.1124/mol.113.088526
This article has not been copyedited and formatted. The final version may differ from this version.

P-gp substrates (Cramer et al., 2007; Gatlik-Landwojtowicz et al., 2006; Schmid et al., 1999) prompted us to investigate the importance of tyrosine hydroxyl groups for interaction with propafenone analogues.

A combination of photolabeling and mass spectrometry recently enabled us to demonstrate a dual interaction mode of P-glycoprotein with substrates in two rotationally symmetric positions. These involve tyrosine residues, which in the present study were mutated to phenylalanine to assess the contribution of tyrosine hydroxyl groups to hydrogen bond formation with propafenone type ligands. Data indicate an important role of these residues for interaction with propafenones, but also with the paradigmatic P-gp substrate rhodamine123 (rh123), thus providing additional experimental evidence for the dual interaction mode of P-gp with solutes and drugs.

Molecular Pharmacology Fast Forward. Published on December 23, 2013 as DOI: 10.1124/mol.113.088526
This article has not been copyedited and formatted. The final version may differ from this version.

Materials and Methods

Sequence Alignments and Homology Modeling. Generation of the ABCB1 model was described previously (Stockner et al., 2009). Briefly, ClustalW was used to obtain multiple sequence alignments of ABCB proteins. The models of human P-gp were based on the crystal structures of the outward facing structure of Sav1866 from *Staphylococcus aureus* and the inward facing structure of ABCB1 from *C. elegans* (PDB ID: 2HYD; 3.0 Å resolution (Dawson and Locher, 2006) and 4F4C; 3.4 Å resolution (Jin et al., 2012)) using MODELLER (version 9v12) (Marti-Renom et al., 2000; Sali and Blundell, 1993). The N-terminus before the elbow helix as observed in the *C. elegans* ABCB1 structure was not included in the model and the interrupted helix 10 was replaced by a de novo model of an ideal helix. This replacement is supported by the observation of a contiguous helix 10 in all other structures from the ABCB transporter family. Initial models were further optimized by relaxation simulations of a membrane inserted transporter.

Knockdown of endogenous P-gp in HEK293 cells

Construction and prevalidation of shRNA Vectors

HEK293 cells endogenously express P-gp at a level corresponding to approximately 5% of transiently expressed protein. In order to avoid interference from endogenous P-gp in functional assays, the transporter was knocked down by transduction with pLKO.1 lentiviral vectors (Moffat et al., 2006) containing P-gp shRNA constructs targeted towards the 3'UTR of the endogenous sequence as described by Addgene (http://www.addgene.org/plko). Briefly, five specific oligonucleotides (Sigma-Aldrich, St. Louis, MO, USA) targeting the 3' UTR of the ABCB1 gene were introduced into the Age I – EcoR I sites of pLKO.1 (Addgene, Cambridge MA, USA, plasmid # 10878).

ABCB1_1_fwd:

ccggAAGAGGTATCTGTTTAACATTctcgagAATGTTAAACAGATACCTCTTttttg

ABCB1_2_fwd:

ccggGAATTATGAAGAGGTATCTGTctcgagACAGATACCTCTTCATAATTCttttg

Molecular Pharmacology Fast Forward. Published on December 23, 2013 as DOI: 10.1124/mol.113.088526
This article has not been copyedited and formatted. The final version may differ from this version.

ABCB1_3_fwd:

ccggGAACAGAGTGAGAGACATCATctcgagATGATGTCTCTCACTCTGTTCttttttg

ABCB1_4_fwd:

ccggGTGGAGAGAAATCATAGTTTActcgagTAAACTATGATTTCTCTCCACttttttg

ABCB1_5_fwd:

ccggGACTGTATGAGATGTTAAATActcgagTATTTAACATCTCATACAGTCttttttg

ABCB1_1_rev:

aattcaaaaaAAGAGGTATCTGTTTAACATTctcgagAATGTTAAACAGATACCTCTT

ABCB1_2_rev:

aattcaaaaaGAATTATGAAGAGGTATCTGTctcgagACAGATACCTCTTCATAATTC

ABCB1_3_rev:

aattcaaaaaGAACAGAGTGAGAGACATCATctcgagATGATGTCTCTCACTCTGTTC

ABCB1_4_rev:

aattcaaaaaGTGGAGAGAAATCATAGTTTActcgagTAAACTATGATTTCTCTCCAC

ABCB1_5_rev:

aattcaaaaaGACTGTATGAGATGTTAAATActcgagTATTTAACATCTCATACAGTC

A non-targeting shRNA vector (Addgene plasmid # 1864) was used as a negative control. All shRNA expression cassettes were verified by sequencing. To test for efficiency and specificity the five candidate shRNA constructs (#1-#5) were analyzed for target mRNA degradation using the Dual-Luciferase Reporter Assay System (Promega, Mannheim, Germany) according to the manufacturer's recommendations. The inhibitory effects generated by shRNA constructs were expressed as normalized ratios between the activities of the reporter luciferase gene (firefly) and the luciferase reporter target gene fusion (renilla) relative to the negative control vector containing scrambled shRNA (Addgene, plasmid # 1864). The two most effective constructs (#1 and #4) targeting endogenous P-gp were used to stably transduce HEK293 cells (see supplementary Fig. 1 for further details).

Viral Particle Production and Target Cell Infection

Molecular Pharmacology Fast Forward. Published on December 23, 2013 as DOI: 10.1124/mol.113.088526
This article has not been copyedited and formatted. The final version may differ from this version.

Described shRNA-pLKO.1 constructs were co-transfected with the packaging plasmid pPax2 (Addgene, plasmid # 12260) and the envelop plasmid pMD2.G (Addgene, plasmid #12259) into human embryonic kidney 293FT cells using Lipofectamine 2000 (Invitrogen, LifeTech Austria, Vienna, Austria). Virus was harvested 72 h post transfection and concentrated using a PEG virus precipitation kit (BioVision, Milpitas, CA, USA). Infections of HEK293 cells were carried out in the presence of 10 µg/ml hexadimethrine bromide (synonym: polybrene, Sigma-Aldrich). Following transduction, cells were selected with 2 µg/ml puromycin.

Construction of P-gp mutants

The following primers were used for generation of the Y307F, Y310F, Y307/Y310F, Y950F, Y953F and Y950F/Y953F mutations of hexa-his tagged human P-gp in the entry vector pENTR4:

Y307F-f 5'- CTTTCCTGCTGATCTTTGCATCTTATGCTCTGGCC-3',

Y307F- r 5'- GGCCAGAGCATAAGATGCAAAGATCAGCAGGAAAG-3',

Y310F-f 5'- CTTTCCTGCTGATCTATGCATCTTTTGCTCTGGCC-3',

Y310F- r 5'- GGCCAGAGCAAAAGATGCATAGATCAGCAGGAAAG-3',

Y307F/Y310F-f 5'- CTTTCCTGCTGATCTTTGCATCTTTTGCTCTGGCC-3',

Y307F/Y310F-r 5'- GGCCAGAGCAAAAGATGCAAAGATCAGCAGGAAAG-3',

Y950F-f 5'- TCACCCAGGCAATGATGTTTTTTTCCTATGCTGGATG-3',

Y950F-r 5'- CATCCAGCATAGGAAAAAAACATCATTGCCTGGGTGA-3',

Y953F-f 5'-ACCCAGGCAATGATGTATTTTTCCTTTGCTGGATGTTTC-3',

Y953F-r 5'- GAAACATCCAGCAAAGGAAAAATACATCATTGCCTGGGT-3',

Y950F/Y953F-f 5'-CCTTCACCCAGGCAATGATGTTTTTTTCCTTTGCTGGATGTTTCC -3',

Y950F/Y953F-r 5'-GGAAACATCCAGCAAAGGAAAAAAACATCATTGCCTGGGTGAAGG-3'.

Further, Q132R and Q773R mutations were introduced to the constructs above by using

Q132R-f 5'- GCTGCTTACATTCGTGTTTCATTTTG-3',

Q132R-r 5'- CAAAATGAAACACGAATGTAAGCAGC-3',

Q773R-f 5'- CATTTTTCCTTCGAGGTTTCACATTTG-3',

Q773R-r 5'- CATTTTTCCTTCGAGGTTTCACATTTG-3'.

Molecular Pharmacology Fast Forward. Published on December 23, 2013 as DOI: 10.1124/mol.113.088526
This article has not been copyedited and formatted. The final version may differ from this version.

Gateway cloning technology (Hartley et al., 2000) was applied to shift the wild type and mutant P-gp constructs to pCEP4 destination vector.

Surface expression of wild type P-gp and mutants

HEK293 cells were transiently transfected with wild type or mutant P-gp constructs using TurboFect transfection reagent (Fisher Scientific, Vienna, Austria) according to the manufacturer`s instructions. Expression was determined by using the mouse monoclonal - P-gp specific - MRK16 antibody (5µg/mL) (Kamiya Biomedical Company, Seattle, WA, USA), IgG2A (2.5 µg/mL) as the control antibody and a Becton Dickinson FACSCalibur flow cytometer (BD Biosciences, Vienna, Austria) as described previously (Parveen et al., 2011).

Continuous monitoring of rhodamine123 zero trans efflux

Cells were trypsinized, centrifuged at 500g and washed with phosphate-buffered saline (PBS). 10^6 cells per data point ($0.5*10^6$/ml) were resuspended in DMEM, pH 7.8 containing rh123 (Sigma-Aldrich, St. Louis, MO) at a final concentration of 0.2 µg/ml (0.53 µmol/l) and incubated at 37ºC under gentle continuous agitation for 30 min. Loading was terminated by chilling tubes on ice and cells were washed twice with ice cold DMEM, pH 7.4. Efflux was initiated by resuspending the cell pellet in DMEM, pH 7.4 prewarmed to 37ºC. Efflux was monitored continuously over five minutes in a Becton Dickinson FACSCalibur flow cytometer at 37°C using a temperature controlled water jacket. Viable cells were selected by setting appropriate gates for forward and side scatter. The excitation and emission wavelengths were 488 nm and 534 nm, respectively. Data points were exported to a graphic user interface (GUI) programmed in LabView 2013 (National Instruments, Salzburg, Austria), which allows the import of flow cytometry standard files. Average MFU values were computed for selected time intervals (default 1 second intervals) and these MFU values were displayed as a function of time. When selecting 1 second intervals, the time course consists of 300 individual data points, each averaging about 3000 gated events. First order rate constants (*k*-values) were calculated from an exponential fit according to the following equation $y=a*e^{-kt}+c$, where *a* is the difference between the zero and infinite time point of the curve, *e* is the Euler number, *k* is the first order rate constant, *t* is the time in seconds and *c*

Molecular Pharmacology Fast Forward. Published on December 23, 2013 as DOI: 10.1124/mol.113.088526
This article has not been copyedited and formatted. The final version may differ from this version.

is the background fluorescence of cells (refer to supplementary Fig.2 for further details). Transport rates were calculated from *k*-values normalized to surface expression, which was determined by MRK16 staining. Fractional transport rates were calculated for each individual experiment.

Inhibition Assays

Cells were loaded with rh123 as described above and the cell pellet was resuspended in medium pre-warmed to 37 °C that contained either no inhibitor or compounds (GPV005, GPV031 or GPV366; refer to supplementary Fig. 3 for structures) at various concentrations ranging from 4.6 nM to 90 µM, depending on solubility and expected potency. Eight concentrations (serial 1:3 dilution) were tested for each propafenone analog. Inhibition of rh123 efflux by these compounds was monitored continuously over five minutes at 37 °C. First order rate constants (k) were plotted as a function of inhibitor concentration and IC_{50} values were calculated for each compound by non-linear regression analysis.

Statistical Analysis

All data are expressed as mean ± standard deviation (SD). Averages of IC_{50} values were compared using one way ANOVA (GraphPad prism software, version 5). Post-hoc Tukey analyses were carried out to find groups whose mean differences were significant.

Molecular Pharmacology Fast Forward. Published on December 23, 2013 as DOI: 10.1124/mol.113.088526
This article has not been copyedited and formatted. The final version may differ from this version.

Results

Selection of residues and design of mutants

Our group previously demonstrated that photoactivated propafenone derivatives label residues in pseudosymmetric position including helices 5 and 11 (Parveen et al., 2011) (Fig 1). These results imply the existence of two substrate-transporter interaction modes. Full transporters have arisen from half transporters by gene duplication. In homodimeric half transporters, each conformation of any set of amino acid residues is represented twice. On theoretical grounds binding of ligands would therefore be possible in either of two modes. In full transporters, these sets of amino acids were reshaped by evolution making them similar, but nonidentical (Parveen et al., 2011). In order to designate sets of interacting amino acid residues, the term “site” will be used subsequently. Please note that it is only meant to refer to sets of ligand-interacting amino acid residues in pseudosymmetric positions of the transporter that might either be separated in space or partially or fully overlapping.

Accordingly, rh123 was shown to prefer the first interaction site (site 1), whereas propafenones, verapamil, and vinblastine have a preference for the second (site 2). Introduction of arginine residues in positions 773 and 132 changes the binding probability for protonatable compounds in site 1 or 2 by charge repulsion. Previous experiments identified site 2 tyrosine residue Y953 in helix 11 as being photolabeled by propafenones (Parveen et al., 2011; Pleban et al., 2005). The conserved residue Y953 is located in a consensus ^{950}Y(F)xSYA^{954} motif that is also found in site 1. This amino acid residue lies at the apex of site 2 (Fig. 1) and represents a potential interaction partner for propafenone type ligands.

Pore exposed tyrosine residue Y950, which lies one helical turn away from Y953 towards the cell interior, was also mutated to phenylalanine as it was considered a potential additional interaction partner for propafenones. This residue is a phenylalanine in some species, but a tyrosine in humans. Interaction of propafenones with the transporter was quantified by exploring the potential of the compounds to inhibit rh123 efflux. This proved necessary,

Molecular Pharmacology Fast Forward. Published on December 23, 2013 as DOI: 10.1124/mol.113.088526
This article has not been copyedited and formatted. The final version may differ from this version.

because propafenone analogs used in this study rapidly diffuse through biomembranes and thus a net transport is not measureable (Schmid et al., 1999).

Position and local geometry of site 2 are illustrated in Fig. 1A and B and compared between the outward (model based on Sav1866 from *S. aureus* (Dawson and Locher, 2006) and the inward facing structures (model based on ABCB1 from *C. elegans* (Jin et al., 2012). The local geometry at site 2 remained remarkably similar between the two structures. We observed a reduction in the distance between transmembrane helices 1 and 12 by approximately 2 Å during the transition from the inward to the outward facing structure, while accessibility to residues Y950 and Y953 was comparable. The hydroxyl functional groups of both tyrosine residues remained water exposed in both conformations and would therefore be able to form hydrogen bonds to a ligand binding to site 2.

Effect of the removal of Y950 and Y953 OH-groups on rhodamine 123 efflux

P-gp mutants were first characterized for their ability to transport rh123 in order to assess any potential effect of changes in its transport rate on evaluation of propafenones. Rh123 is a preferred site 1 substrate, but also transported *via* site 2. First order rate constants *k* were normalized by expression to account for differences in the amount of protein present at the plasma membrane, which differs as a result of using a transient expression system (refer to supplementary Fig. 4 for the linear relationship between first order rate constants and expression). The (normalized) transport rates are therefore independent of the amount of protein expressed. All mutants were detected at the plasma membrane, though the expression levels of Q132R/Y950F, Q773R/Y950F and Y307F/Y310F were reduced (supplementary Fig. 5). Correct formation of the contact interfaces between helices 2/11 and 5/8 is an important requirement for proper engagement of coupling helices 2 and 4 into the sockets formed between the core and the alpha-helical domain of NBD1 and NBD2, respectively. Less efficient folding of these mutants, which reside in the 2/11 and 5/8 interfaces, is likely the cause of lower plasma membrane expression.

Molecular Pharmacology Fast Forward. Published on December 23, 2013 as DOI: 10.1124/mol.113.088526
This article has not been copyedited and formatted. The final version may differ from this version.

Mutant Y950F showed a similar transport rate as wild type protein, while mutant Y953F showed a significantly decreased rate (54 ± 12% of wild type) (Fig. 2). The double mutant Y950F/Y953F showed a decrease that was comparable to that observed for the Y953F single mutant alone. Thus only the OH-group of residue Y953, but not that of Y950 contributes to rh123 transport.

Access of rh123 to binding site 1 and 2 can be controlled by the introduction of positive charges (arginines) in the access path to the ligand binding sites. We have previously shown that the Q132R mutation blocks access to site 2 for rh123, while the Q773R mutation prevents rh123 access to site 1 (Parveen et al., 2011). The effect of the Y953F mutation on rh123 efflux should be abolished by introducing selector residue R132 and be more pronounced when deselecting site 1 by introducing selector residue R773. Introduction of arginine residues in positions 132 or 773 led to a decrease in rh123 efflux to 75 ± 11% and 37 ± 8% of wild type, respectively (Fig. 2). These data are in agreement with our previous results, in which the same rank order of transport activity was found. As expected, presence of the selector residue R132 abrogated the effect of single and double tyrosine mutation on transport activity. This is illustrated by comparable transport activity of the Q132R/Y950F, Q132R/953F and Q132R/Y950F/Y953F mutants. These results also demonstrate that Y to F mutations in positions 950 and 953 do not perturb protein mechanics. This is an important finding, because impairment of function is a frequently encountered limitation of site directed mutagenesis (Ito et al., 2001; Koike et al., 2002; Swartz et al., 2013).

In contrast, transport rates were found to be lower in the Q773R/Y953F mutant as compared to the Q773R mutant alone, though this decrease did not reach statistical significance. Definitely, no decrease in transport activity was observed for the Y950F mutant introduced in the R773 background. In summary, these results demonstrate that the hydroxyl group of residue 953, but not that of 950, plays a role for rh123 transport.

Interestingly, neither single nor double mutation of corresponding residues Y307 and Y310 in binding site 1 changed rh123 efflux (supplementary Fig. 6). These findings indicate that

Molecular Pharmacology Fast Forward. Published on December 23, 2013 as DOI: 10.1124/mol.113.088526
This article has not been copyedited and formatted. The final version may differ from this version.

hydrogen bonding interactions are of minor importance for interaction of rh123 with tyrosines located on helix 5. This clearly reflects evolutionary divergence of the two sites. While aromatic interactions likely are important, these were not subject of the present study.

Role of Y950 and Y953 for the formation of hydrogen bonds with propafenone analogues

Protonatable propafenones GPV005 and GPV031 were chosen to be studied with wild type protein and in the R132 background. The non-protonatable acid amide GPV366 served as a control that is not influenced by the selector residue R132. Representative examples of concentration response curves for compound GPV005 are shown for wild type, single and double tyrosine mutants (Fig. 3A). Wild type showed an IC_{50} value of 518 ± 141 nM, while the values for the single mutants Y950F and Y953F were 1348 ± 229 and 1207 ± 362 nM, respectively. The double mutant had an IC_{50} value of 2418 ± 194 nM (Fig. 3B, refer to Table 1 of the supplemental material for numerical values and Tables 2A and 2B for statistical significance of differences in IC_{50} values). An analogous pattern was seen for GPV031 (wild type: 85 ± 22 nM, Y950F: 238 ± 84 nM, Y953F: 287 ± 109 nM, Y950F/Y953F: 630 ± 87 nM) (Fig. 3C). The fold change in IC_{50} values was thus similar for both compounds. Data suggest H-bonding interactions of compounds with both tyrosine OH-groups, because a comparable increase in IC_{50} values was observed for each of them and an additive effect was seen when both of them were mutated. Fig. 3D and supplementary Table 1 summarize data for the non-protonatable acid amide GPV366. In contrast to protonatable propafenones, a higher IC_{50} value was observed for the Y953F, but not for the Y950F single mutant. The fold change for the double mutant was comparable to that observed for the Y953F single mutant (wild type: 2239 ± 391 nM, Y950F: 2984 ± 79 nM (n.s.), Y953F: 15946 ± 2941 nM (7.1 fold change relative to wild type), Y950F/Y953F: 17819 ± 2106 nM (8 fold change).

Effect of site 2 tyrosine mutants in the R132 background

The at least 3-fold difference in IC_{50} values for wild type protein (GPV005: 518 ± 141 nM, GPV031: 85 ± 22 nM) (Fig. 3B, C) and the Q132R mutant (GPV005: 1414 ± 215 nM,

Molecular Pharmacology Fast Forward. Published on December 23, 2013 as DOI: 10.1124/mol.113.088526
This article has not been copyedited and formatted. The final version may differ from this version.

GPV031: 521 ± 183 nM) (Fig. 4A, B) demonstrates that an arginine residue in position 132 prevents access of protonatable compounds to site 2. Introducing tyrosine mutations in the R132 background should in principle make IC_{50} values of protonatable compounds independent of the presence of site 2 mutations. Indeed data in Fig. 4A, B and supplementary Table 1 show that for the Q132R/Y950F mutant IC_{50} values were similar to those observed in the Q132R background alone. However IC_{50} values were still higher in the Q132R/Y953F mutation. This increase was not significant for GPV005, but reached significance for GPV031. Thus, removal of the hydroxyl group of tyrosine 953 still affected IC_{50} values of protonatable propafenones, indicating that protonatable compounds were still able to access site 2, even though to a lesser extent. Incomplete prevention of access is a result of ligand properties and not the transporter itself, because both, GPV005 and GPV031 have a pKa (Ecker et al., 1999), which results in charged and uncharged species to coexist under physiological conditions (further details are given in the discussion section).

For the non-protonatable acid amide GPV366 a higher IC_{50} value was observed in the Q132R/Y953F mutant (Q132R: 1074 ± 282 nM, Q132R/Y953F: 3261 ± 965 nM), while the Y950F mutation in the same background did not affect potency (966 ± 259 nM) (Fig. 4C). Although the pattern was similar to that observed in the wild type background, the fold change was lower in the Q132R background and the IC_{50} value was somewhat lower in the protein containing the Q132R mutation than for wild type. A possible explanation for this effect is the lack of competition of GPV366 in the preferred binding site 2 with rh123, because rh123 binding to site 2 is abolished by the Q132R mutation.

The higher IC_{50} values in the Q132R/Y950F/Y953F were not due to an additive effect of the two tyrosine mutations on binding of propafenones. Therefore the observed effect cannot be explained by a contribution from tyrosine mutations on small molecule binding and therefore has to have other reasons. Certainly, the effect is not brought about by a global perturbance of protein structure and function, because the Q132R mutant and the Q132R/Y950F/Y953F triple mutant showed comparable rh123 transport rates (*cf*. Fig. 2). All three mutations are

Molecular Pharmacology Fast Forward. Published on December 23, 2013 as DOI: 10.1124/mol.113.088526
This article has not been copyedited and formatted. The final version may differ from this version.

located at the contact interface of helices 2 and 11 and might thus locally influence the geometry of binding site 2 in the triple mutant. Importantly, this effect does not have a bearing on the interpretation of results in this study.

Molecular Pharmacology Fast Forward. Published on December 23, 2013 as DOI: 10.1124/mol.113.088526
This article has not been copyedited and formatted. The final version may differ from this version.

Discussion

The presence of tyrosines in binding cavities is important both for specificity and affinity of solutes towards proteins (Koide and Sidhu, 2009). This has been illustrated for a number of bacterial, rodent and human transporters. The importance of tyrosine residues for the interaction of the bacterial exporter QacA from *Staphylococcus aureus* with solutes was studied by Wu *et al* (Wu et al., 2008). Mutation of residue Y410 in the drug binding pocket to phenylalanine led to a decrease in the transport rate of QacA for several substrates, including monovalent dyes. A study on the human ABCC1 transporter (multidrug resistance protein, MRP1) found that mutation of two cytoplasmic loop tyrosines (Y1189 and Y1190) to alanine or serine, respectively, resulted in a 50% reduced transport rate for different organic anion substrates, particularly glutathione (Conseil et al., 2005). Mammalian ABC transporters are rich in aromatic residues in the apical region of the central cavity as illustrated by the crystal structure of mouse ABCB1, protein homology models of human ABCB1 and the related human hepatic transporter ABCB4 (Gutmann et al., 2010), as well as the crystal structure of ABCB10 (Shintre et al., 2013). Interactions formed at the apex of the central cavity may be a prerequisite for substrate induced nucleotide occlusion in one of the composite nucleotide binding site, which in turn affords the outward facing conformation and substrate release (Sauna et al., 2007; Tombline et al., 2006; Tombline et al., 2005).

Our study of the importance of the hydrogen-bonding capability of Y950 and Y953 was motivated by three lines of evidence: (i) the critical role that tyrosines play in molecular recognition, (ii) the projected location of these residues in binding site 2 and (iii) the presence of a conserved Y(F)xSYA motif, in which the second tyrosine is photolabeled by propafenones (Parveen et al., 2011). Residue Y953 seems to be highly conserved in multiple sequence alignments of annotated P-gp orthologs, while substitutions of Y950 by phenylalanine are more frequent.

In order to address the role of H-bonding interactions of these two tyrosines for rh123 efflux, the transport rate of this preferred site 1 substrate was determined either in wild type or the

Molecular Pharmacology Fast Forward. Published on December 23, 2013 as DOI: 10.1124/mol.113.088526
This article has not been copyedited and formatted. The final version may differ from this version.

respective selector mutation background. Residues Q132 and Q773 are located below and outside the binding sites, and replacement by arginine was previously shown to direct protonatable compounds away from one and towards the respective alternate site by charge repulsion. Experimental evidence indicates Y953 to represent an H-bonding partner for rh123, because a significant decrease in transport rates in wild type and the Q773R backgrounds was observed. Identical transport rates were found for the mutant Q132R and the Y953F mutant in the Q132R background. This finding was expected, because (i) rh123 always carries one positive charge at physiological pH (Shinomiya et al., 1992) and (ii) introducing selector residue R132 would abolish any influence that mutations in the site, which is now inaccessible for ligands, would have.

For reasons detailed in the results section, hydrogen bonding interactions of tyrosines with propafenone analogs GPV005, GPV031 and GPV366 were assessed by determining IC_{50} values for rh123 efflux inhibition. Both residues Y950 and Y953 were demonstrated to play a role as hydrogen bonding partners for the protonatable propafenones GPV005 and GPV031, whereby the effect was additive in the double mutant. GPV366 showed a hydrogen bonding interaction with residue Y953, while residue Y950 did not contribute. As expected, the double mutant showed an IC_{50} value that was comparable to that of the Y953F mutant.

In principle, access of charged propafenones to preferred site 2 should be prevented by introduction of the selector mutation R132. IC_{50} values were therefore expected to be the same in single and double tyrosine mutants generated in the Q132R background. Indeed no difference was observed between the Q132R single and the Q132R/Y950F double mutant. However, higher IC_{50} values were found for the Y953F mutant, though less pronounced than in the wild type background. These results indicate that propafenones can still reach site 2. Propafenones coexist in protonated and non-protonated forms at physiological pH. The uncharged ligand species can still have access to site 2, which has been deselected for the protonated ligand species by introducing the Q132R mutation. The permanently charged rh123 is entirely prevented from reaching site 2 by introducing selector residue R132. The

Molecular Pharmacology Fast Forward. Published on December 23, 2013 as DOI: 10.1124/mol.113.088526
This article has not been copyedited and formatted. The final version may differ from this version.

pKa value of GPV005 is 8.4 and that of GPV031 is 7.3 (Ecker et al., 1999). This allows estimating the percentage of protonated species of GPV005 and GPV031 at intracellular pH. Accordingly, the charged species amounts to >90% and 60-70%, respectively. GPV005 would therefore be prevented from accessing site 2 to a larger extent than GPV031. Indeed results in Fig. 4A and B show that this is the case. For GPV005 mutant Q132R/Y953F showed a 1.5 fold higher IC_{50} value than the Q132R mutation, while the fold change for GPV031 was 2.1 fold and that for uncharged GPV366 was 3.0 fold. From experiments in the wild type background (Fig. 3), an equal contribution of residues Y950 and Y953 was expected. However, such an effect was not observed in the Q132R background (Figs. 4A and B). Residue Y950 thus lost its importance as an interaction partner, possibly due to the close proximity of residues Q132R and Y950, which are predicted in models to have a C-alpha distance of approximately 7 Å. Though residue Q132 has been shown not to be a direct interaction partner for propafenone type ligands (Parveen et al, 2011), a steric effect of the arginine side chain is likely, but only seen for those propafenone analogs that interact with Y950 (GPV005, GPV031, not GPV366).

The triple Q132R/Y950F/Y953F mutant showed a further increase in IC_{50} values for all compounds, which is obviously not due to interaction with tyrosines. As discussed in the results section, this finding is hypothesized to be due to local changes in site 2. The fact that the extent of deselecting inversely correlates with the fold change (2.3 fold for GPV005, 2.7 fold for GPV031 and 4.9 fold for GPV366) is supporting this hypothesis.

Interaction of propafenones with the transporter was assessed by determining IC_{50} values for rh123 efflux inhibition. In these experiments, both the interaction of P-gp with rh123 and with propafenones contributes to the outcome of the experiments. We therefore addressed the question if a change in rh123 efflux would affect propafenone IC_{50} values in the way we observed. When the transporter is partially impaired, an inhibition should be easier to accomplish. In contrast, our experiments showed the inverse, i.e. an increase in IC_{50} values, rather than a decrease. Therefore the effects seen for the mutants are certainly not due to

Molecular Pharmacology Fast Forward. Published on December 23, 2013 as DOI: 10.1124/mol.113.088526
This article has not been copyedited and formatted. The final version may differ from this version.

the observed decrease in rh123 flux, because in that case they should be the opposite of what we observed.

Fig. 5 summarizes results in a schematic way. Tyrosines are shown in yellow, when found important for H-bond formation and in gray, when not. Tyrosines Y950 and Y953 are H-bonding with protonatable compounds GPV005 and GPV031 (panel A), while only residue Y953 is important for interaction with the non-protonatable acid amide GPV366 (panel B). When the wild type glutamine in position 132 is replaced by arginine, the probability of protonatable compounds to reach site 2 is decreased. This is indicated by gray font color of compounds GPV005 and GPV031. Also residue Y950 loses its importance as a residue that forms H-bonds with propafenones (panel C). Compound GPV366 only interacts with residue Y953 (panel D).

Our results are in agreement with earlier work on tyrosine residues in mouse and human P-gp. These previous studies evaluated toxicity (a composite of the influence of mutation on trafficking and function) (Hanna et al., 1996) and ATPase activity of reconstituted P-gp (Loo and Clarke, 2000), respectively. A direct evaluation of transport activity has not been performed in earlier work. Philippe Gros' group studied alanine mutants of tyrosine residues Y946 and Y949 in mouse mdr3. These residues are found in analogous position to tyrosines Y950 and Y953 in the human sequence. The ability of mutants to confer resistance to actinomycin D, adriamycin, colchicine and vinblastine was determined. In these experiments mutations to alanine probed for both H-bonding and aromatic interactions. The Y949A mutation increased colchicine and adriamycin toxicity, the Y946A made cells more sensitive to vinblastine, while both mutants increased sensitivity towards actinomycin D. These data are in agreement with the finding that drugs, which we previously found to preferentially bind to site 1 or site 2, respectively, are affected by mutation of tyrosines. Loo and Clarke demonstrated altered ATPase stimulation of the human protein for the Y953A mutant by verapamil, colchicine and vinblastine, but did not present evidence for a direct involvement in drug binding.

Molecular Pharmacology Fast Forward. Published on December 23, 2013 as DOI: 10.1124/mol.113.088526
This article has not been copyedited and formatted. The final version may differ from this version.

Conclusions

A dual substrate binding mode is rooted in the rotational C2 symmetry of human ABC transporters. In this manuscript, the contribution of active site tyrosine residues for substrate interaction with propafenones has been studied with respect to their preferred interaction site 2. Propafenones were used as model compounds because of the availability of photolabeling data, which previously showed a dual pseudosymmetric mode of interaction with P-glycoprotein. The photolabeled tyrosine residue Y953 is shown to form hydrogen bonds with protonatable and non-protonatable propafenones, but also with preferred site 1 substrate rh123. We provide proof of principle that the preferred propafenone binding site can be studied individually and the influence of mutation can be resolved in a site specific manner. We believe that dual symmetry related sites present in other human ABC exporters may potentially be linked to disease etiologies. One candidate is the human bile salt export pump, which specifically transports conjugated bile acids, but at the same time is inhibited by numerous systemically administered drugs.

Molecular Pharmacology Fast Forward. Published on December 23, 2013 as DOI: 10.1124/mol.113.088526
This article has not been copyedited and formatted. The final version may differ from this version.

Authorship contributions

Participated in research design: Dönmez Cakil, Stockner, Chiba

Conducted experiments: Dönmez Cakil, Khunweeraphong, Parveen, Artaker, Stockner

Contributed new reagents or analytic tools: Pusch, Schmid

Performed data analysis: Dönmez Cakil, Stockner, Chiba

Wrote or contributed to writing of the manuscript: Dönmez Cakil, Sitte, Ecker, Stockner, Chiba

Molecular Pharmacology Fast Forward. Published on December 23, 2013 as DOI: 10.1124/mol.113.088526
This article has not been copyedited and formatted. The final version may differ from this version.

References

Conseil G, Deeley RG and Cole SP (2005) Role of two adjacent cytoplasmic tyrosine residues in MRP1 (ABCC1) transport activity and sensitivity to sulfonylureas. *Biochem Pharmacol***69**(3): 451-461.

Cramer J, Kopp S, Bates SE, Chiba P and Ecker GF (2007) Multispecificity of drug transporters: probing inhibitor selectivity for the human drug efflux transporters ABCB1 and ABCG2. *ChemMedChem***2**(12): 1783-1788.

Dawson RJ and Locher KP (2006) Structure of a bacterial multidrug ABC transporter. *Nature***443**(7108): 180-185.

Ecker G, Huber M, Schmid D and Chiba P (1999) The importance of a nitrogen atom in modulators of multidrug resistance. *Mol Pharmacol***56**(4): 791-796.

Gatlik-Landwojtowicz E, Aanismaa P and Seelig A (2006) Quantification and characterization of P-glycoprotein-substrate interactions. *Biochemistry***45**(9): 3020-3032.

Giacomini KM, Huang SM, Tweedie DJ, Benet LZ, Brouwer KL, Chu X, Dahlin A, Evers R, Fischer V, Hillgren KM, Hoffmaster KA, Ishikawa T, Keppler D, Kim RB, Lee CA, Niemi M, Polli JW, Sugiyama Y, Swaan PW, Ware JA, Wright SH, Yee SW, Zamek-Gliszczynski MJ and Zhang L (2010) Membrane transporters in drug development. *Nat Rev Drug Discov***9**(3): 215-236.

Gutmann DA, Ward A, Urbatsch IL, Chang G and van Veen HW (2010) Understanding polyspecificity of multidrug ABC transporters: closing in on the gaps in ABCB1. *Trends Biochem Sci***35**(1): 36-42.

Hanna M, Brault M, Kwan T, Kast C and Gros P (1996) Mutagenesis of transmembrane domain 11 of P-glycoprotein by alanine scanning. *Biochemistry***35**(11): 3625-3635.

Hartley JL, Temple GF and Brasch MA (2000) DNA cloning using in vitro site-specific recombination. *Genome Res***10**(11): 1788-1795.

Ito K, Oleschuk CJ, Westlake C, Vasa MZ, Deeley RG and Cole SP (2001) Mutation of Trp1254 in the multispecific organic anion transporter, multidrug resistance protein 2 (MRP2) (ABCC2), alters substrate specificity and results in loss of methotrexate transport activity. *J Biol Chem***276**(41): 38108-38114.

Jin MS, Oldham ML, Zhang Q and Chen J (2012) Crystal structure of the multidrug transporter P-glycoprotein from Caenorhabditis elegans. *Nature***490**(7421): 566-569.

Koide S and Sidhu SS (2009) The importance of being tyrosine: lessons in molecular recognition from minimalist synthetic binding proteins. *ACS Chem Biol***4**(5): 325-334.

Koike K, Oleschuk CJ, Haimeur A, Olsen SL, Deeley RG and Cole SP (2002) Multiple membrane-associated tryptophan residues contribute to the transport activity and substrate specificity of the human multidrug resistance protein, MRP1. *J Biol Chem***277**(51): 49495-49503.

Linton KJ, Zolnerciks JK and Schmitt L (2011) *The ABC Transporters of Human Physiology and Disease: Genetics and Biochemistry of ATP Binding Cassette Transporters*, World Scientific Publishing, London.

Liu M, Hou T, Feng Z and Li Y (2013) The flexibility of P-glycoprotein for its poly-specific drug binding from molecular dynamics simulations. *J Biomol Struct Dyn***31**(6): 612-629.

Loo TW and Clarke DM (2000) Identification of residues within the drug-binding domain of the human multidrug resistance P-glycoprotein by cysteine-scanning mutagenesis and reaction with dibromobimane. *J Biol Chem***275**(50): 39272-39278.

MacCallum JL, Bennett WF and Tieleman DP (2007) Partitioning of amino acid side chains into lipid bilayers: results from computer simulations and comparison to experiment. *J Gen Physiol***129**(5): 371-377.

Marti-Renom MA, Stuart AC, Fiser A, Sanchez R, Melo F and Sali A (2000) Comparative protein structure modeling of genes and genomes. *Annu Rev Biophys Biomol Struct***29**: 291-325.

Mian IS, Bradwell AR and Olson AJ (1991) Structure, function and properties of antibody binding sites. *J Mol Biol***217**(1): 133-151.

Moffat J, Grueneberg DA, Yang X, Kim SY, Kloepfer AM, Hinkle G, Piqani B, Eisenhaure TM, Luo B, Grenier JK, Carpenter AE, Foo SY, Stewart SA, Stockwell BR, Hacohen N, Hahn WC, Lander ES, Sabatini DM and Root DE (2006) A lentiviral RNAi library for human and mouse genes applied to an arrayed viral high-content screen. *Cell***124**(6): 1283-1298.

Pace CN, Horn G, Hebert EJ, Bechert J, Shaw K, Urbanikova L, Scholtz JM and Sevcik J (2001) Tyrosine hydrogen bonds make a large contribution to protein stability. *J Mol Biol***312**(2): 393-404.

Parveen Z, Stockner T, Bentele C, Pferschy S, Kraupp M, Freissmuth M, Ecker GF and Chiba P (2011) Molecular dissection of dual pseudosymmetric solute translocation pathways in human P-glycoprotein. *Mol Pharmacol***79**(3): 443-452.

Pleban K, Kopp S, Csaszar E, Peer M, Hrebicek T, Rizzi A, Ecker GF and Chiba P (2005) P-glycoprotein substrate binding domains are located at the transmembrane domain/transmembrane domain interfaces: a combined photoaffinity labeling-protein homology modeling approach. *Mol Pharmacol***67**(2): 365-374.

Sali A and Blundell TL (1993) Comparative protein modelling by satisfaction of spatial restraints. *J Mol Biol***234**(3): 779-815.

Sauna ZE, Kim IW, Nandigama K, Kopp S, Chiba P and Ambudkar SV (2007) Catalytic cycle of ATP hydrolysis by P-glycoprotein: evidence for formation of the E.S reaction intermediate with ATP-gamma-S, a nonhydrolyzable analogue of ATP. *Biochemistry***46**(48): 13787-13799.

Schmid D, Ecker G, Kopp S, Hitzler M and Chiba P (1999) Structure-activity relationship studies of propafenone analogs based on P-glycoprotein ATPase activity measurements. *Biochem Pharmacol***58**(9): 1447-1456.

Shinomiya N, Tsuru S, Katsura Y, Sekiguchi I, Suzuki M and Nomoto K (1992) Increased mitochondrial uptake of rhodamine 123 by CDDP treatment. *Exp Cell Res***198**(1): 159-163.

Shintre CA, Pike AC, Li Q, Kim JI, Barr AJ, Goubin S, Shrestha L, Yang J, Berridge G, Ross J, Stansfeld PJ, Sansom MS, Edwards AM, Bountra C, Marsden BD, von Delft F, Bullock AN, Gileadi O, Burgess-Brown NA and Carpenter EP (2013) Structures of ABCB10, a human ATP-binding cassette transporter in apo- and nucleotide-bound states. *Proc Natl Acad Sci U S A***110**(24): 9710-9715.

Stockner T, de Vries SJ, Bonvin AM, Ecker GF and Chiba P (2009) Data-driven homology modelling of P-glycoprotein in the ATP-bound state indicates flexibility of the transmembrane domains. *FEBS J***276**(4): 964-972.

Swartz DJ, Weber J and Urbatsch IL (2013) P-glycoprotein is fully active after multiple tryptophan substitutions. *Biochim Biophys Acta***1828**(3): 1159-1168.

Tombline G, Donnelly DJ, Holt JJ, You Y, Ye M, Gannon MK, Nygren CL and Detty MR (2006) Stimulation of P-glycoprotein ATPase by analogues of tetramethylrosamine: coupling of drug binding at the "R" site to the ATP hydrolysis transition state. *Biochemistry***45**(26): 8034-8047.

Tombline G, Muharemagic A, White LB and Senior AE (2005) Involvement of the "occluded nucleotide conformation" of P-glycoprotein in the catalytic pathway. *Biochemistry***44**(38): 12879-12886.

Wu J, Hassan KA, Skurray RA and Brown MH (2008) Functional analyses reveal an important role for tyrosine residues in the staphylococcal multidrug efflux protein QacA. *BMC Microbiol***8**: 147.

Molecular Pharmacology Fast Forward. Published on December 23, 2013 as DOI: 10.1124/mol.113.088526
This article has not been copyedited and formatted. The final version may differ from this version.

Footnotes

This research was supported by grants from the Austrian Science Fund FWF [stand alone project 23319, Special Research Fund 35-3509]; and the European Cooperation in Science and Technology [e-COST Action CM0902]. NK acknowledges receipt of a scholarship from the Austrian Federal Ministry of Science and Research (BMWF).

Molecular Pharmacology Fast Forward. Published on December 23, 2013 as DOI: 10.1124/mol.113.088526
This article has not been copyedited and formatted. The final version may differ from this version.

Figure legends:

Figure 1: Location of site 1 (orange; preferred rh123 site) and site 2 (green; preferred propafenone, verapamil and vinblastine site) are indicated in the homology models of P-gp. Panel A shows their location in the outward facing P-glycoprotein structure and in a close up of site 2 in a 90º rotated transporter. Site 2 is viewed from the pore. Residues Q773 (orange) and Q132 (green) lie proximal in the path taken by transported compounds. When mutated to arginine, these residues decrease the binding probability of protonatable compounds in either of the two sites. Panel B shows the same representation of overall structure and a close up of site 2 for the inward facing conformation. Panel C shows the sequence alignment of helices 5 and 11 of P-gp. The cyan box shows the conserved Y(F)xSYA motif, yellow boxes highlight mutated residues tyrosine Y950 and Y953. Residues which were previously shown to be strongly labeled by photoactivated propafenones are indicated in magenta.

Figure 2: Bar graph showing changes in the fractional transport rate of mutants in comparison with wild type. Rh123 efflux was monitored continuously for 5 min. First order rate constants (k) were calculated from an exponential fit and normalized to surface expression that was determined by MRK16 staining. Q773/Y950F/Y953F was expressed at the surface, but no rh123 efflux was detectable. Each value represents the mean ± SD of at least 3 independent experiments (*p< 0.05, ** p< 0.01 ***p< 0.001 compared with wild type P-gp).

Figure 3: Inhibition of rh123 efflux was measured in the absence and presence of 8 serial dilutions of GPV005. Wild type: open diamonds; Y950F/Y953F: filled circles; Y950F: triangles; Y953F: squares (A). IC_{50} values for GPV005 (B), GPV031 (C) and GPV366 (D) were determined by fitting hyperbolic concentration response curves to data points by non-linear regression analysis and calculation of 50% occupancy values. Mean ± SD were calculated from at least 3 independent experiments (*p< 0.05, **p< 0.01 ***p< 0.001 compared with wild type P-gp).

Molecular Pharmacology Fast Forward. Published on December 23, 2013 as DOI: 10.1124/mol.113.088526
This article has not been copyedited and formatted. The final version may differ from this version.

Figure 4: Same as Fig. 3, but tyrosine mutants generated in the Q132R mutation background. Mean ± SD were calculated from at least 3 independent experiments. GPV005 (A), GPV031 (B) and GPV366 (C) (*p< 0.05, **p< 0.01 ***p< 0.001 compared with Q132R mutation).

Figure 5: Schematic presentation of the importance of tyrosine hydroxyl groups (tyrosines; yellow) for interaction with propafenone analogs in the outward facing P-glycoprotein structure (template *Sav1866*) panel A and B; Cα atom of residue Q132 shown as a green sphere) and after introduction of the R132 selector mutation (panel C and D; Cα atom of residue Q132 shown in magenta). The hydroxyl-groups of both Y950 and Y953 are able to form hydrogen bonds with protonatable propafenones GPV005 and GPV031 (A), while compound GPV366 only forms hydrogen bonds with residue Y953 (B). The gray color of residue Y950 and red bar indicate that hydrogen bonds of residue Y950 are not important for interaction. The presence of the selector residue R132 (panel C, D) eliminates the importance of the hydroxyl group of Y950 for propafenone analog binding, while the interaction of residue Y953 continues to contribute to the interaction. Use of grey font color indicates incomplete prevention of access of compounds GPV005 and GPV031 in panel C.

Figure 1

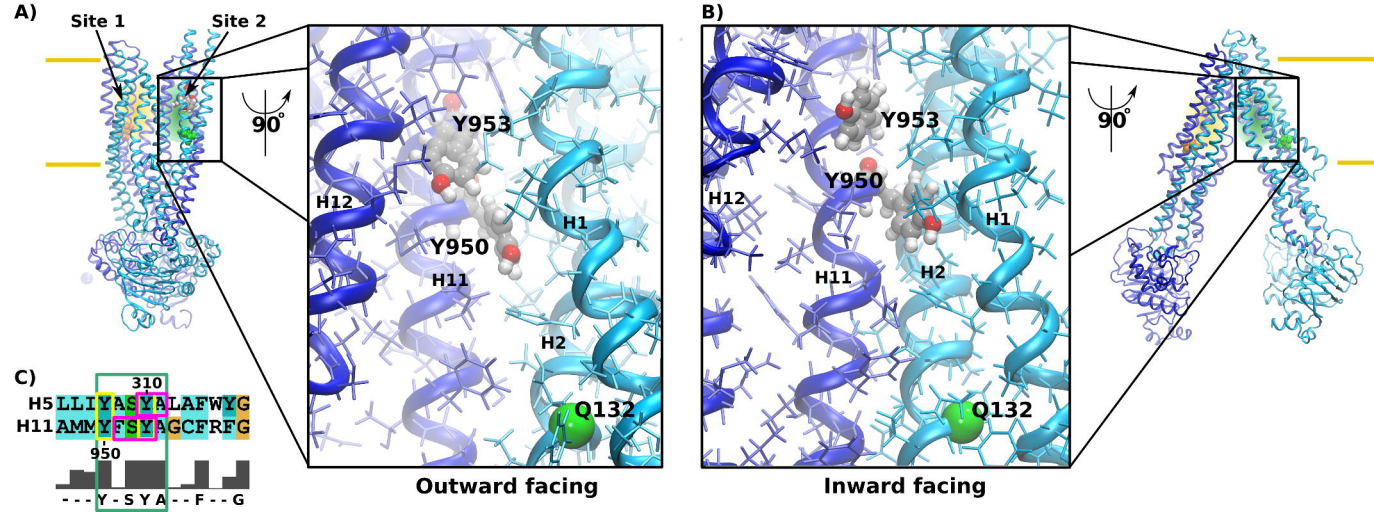
A)
Site 1
Site 2
90°
Y953
H12
H1
Y950
H11
H2
Q132
Outward facing
B)
Y953
Y950
H12
H1
H11
H2
90°
Q132
Inward facing
C)
310
H5 LLIYASYALAFWYG
H11 AMMYFSYAGCFRFG
950
- - - Y - S Y A - - F - - G

Figure 2

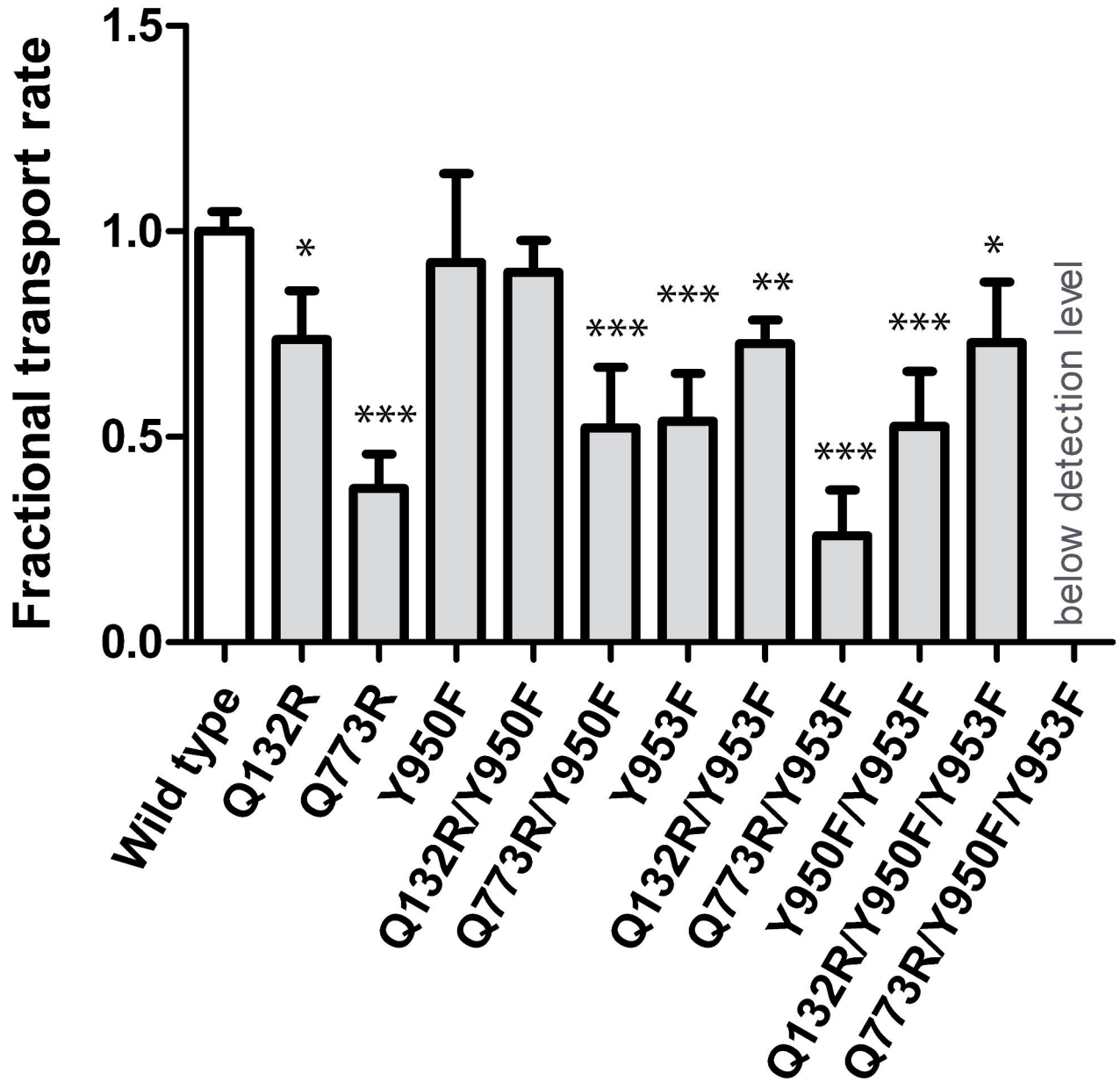
Fractional transport rate
1.5
1.0
0.5
0.0
*
***
***
***
**
***
*
below detection level
Wild type
Q132R
Q773R
Y950F
Q132R/Y950F
Q773R/Y950F
Y953F
Q132R/Y953F
Q773R/Y953F
Y950F/Y953F
Q132R/Y950F/Y953F
Q773R/Y950F/Y953F

Molecular Pharmacology Fast Forward. Published on December 23, 2013 as DOI: 10.1124/mol.113.088526
This article has not been copyedited and formatted. The final version may differ from this version.

Figure 3

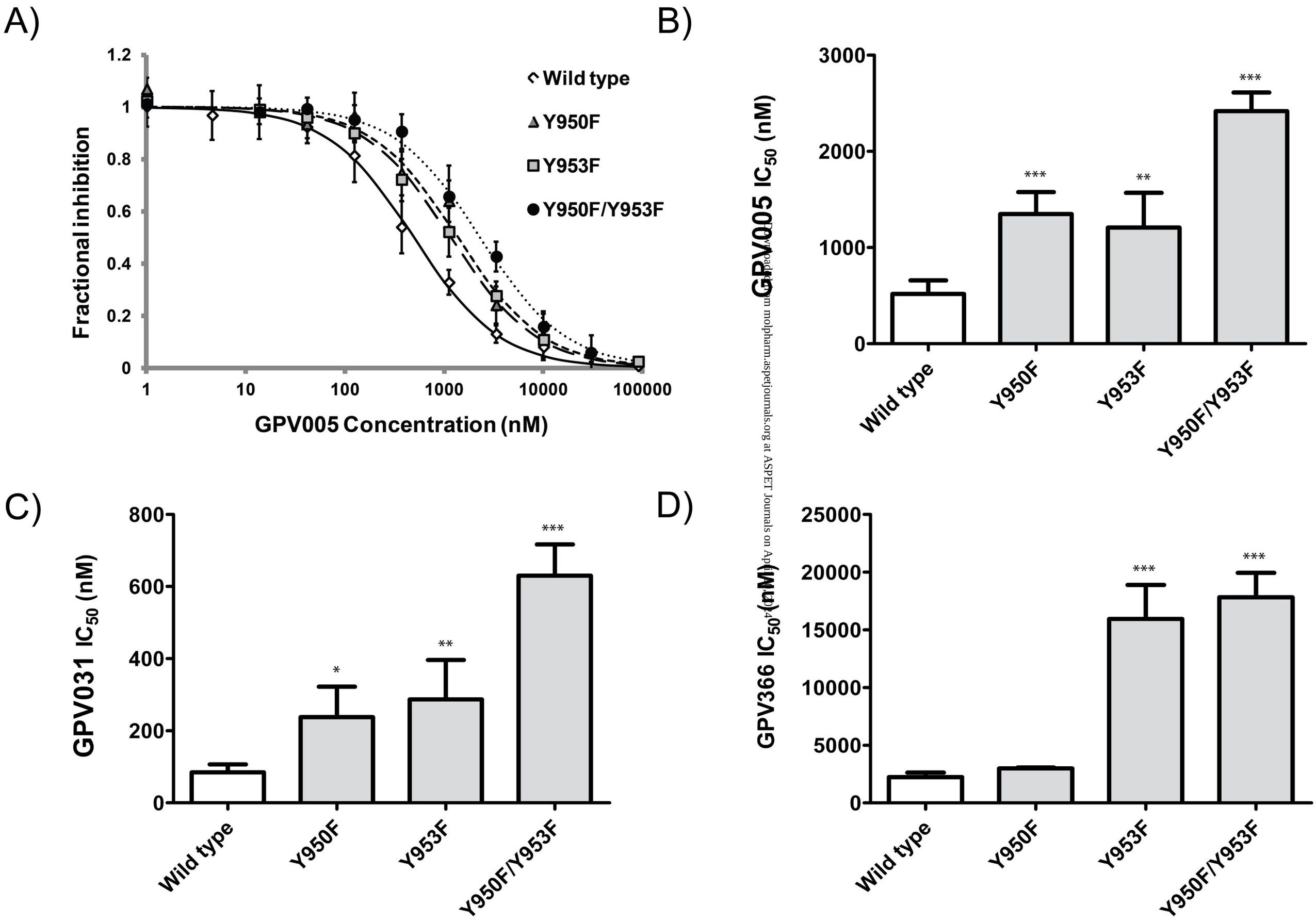

Figure 4

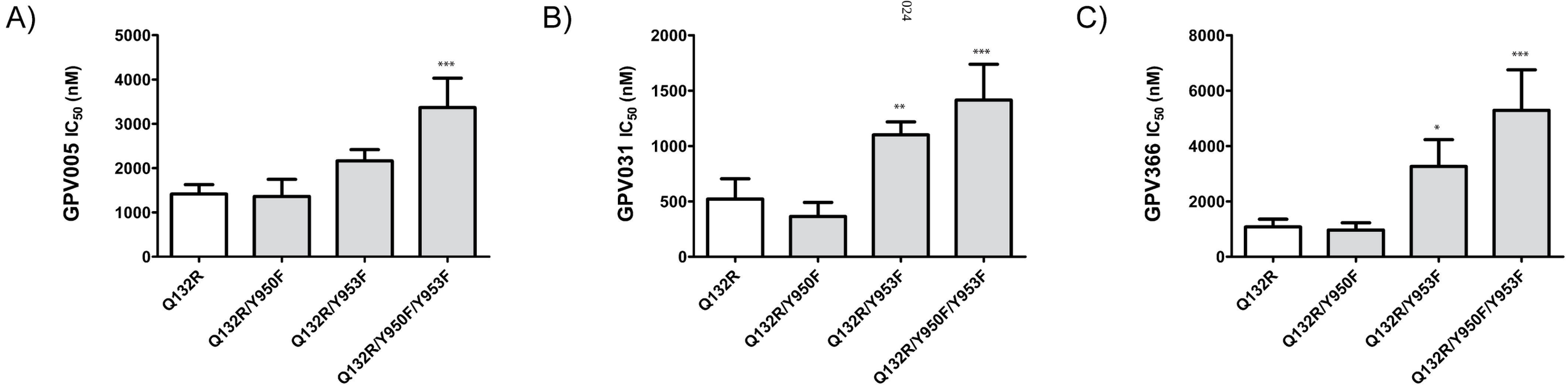

Figure 5

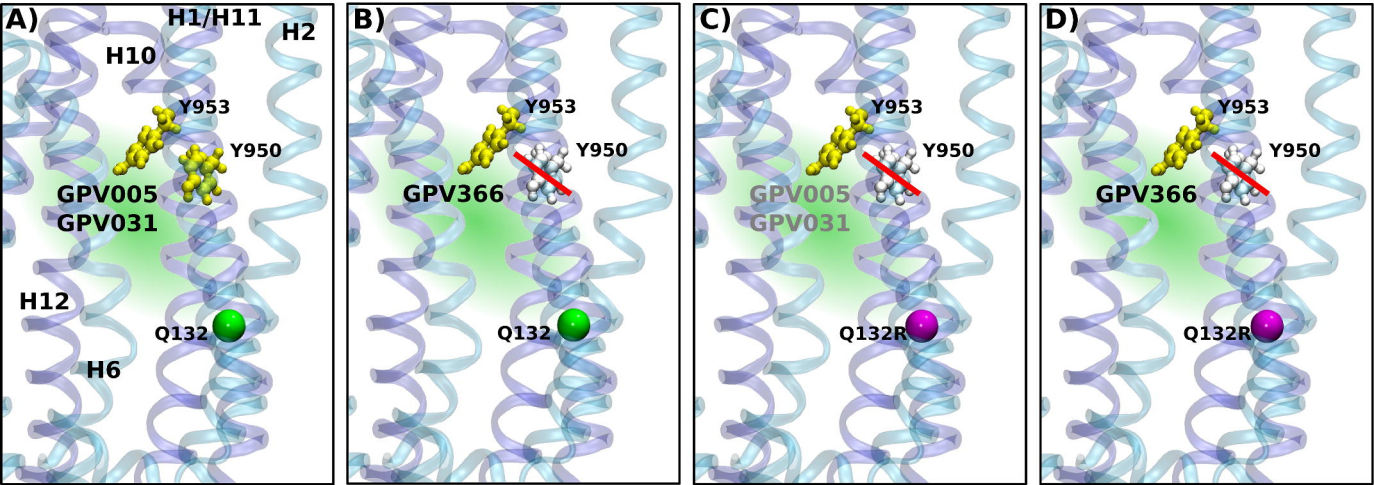
A)
H1/H11
H2
H10
Y953
Y950
GPV005
GPV031
H12
Q132
H6
B)
Y953
Y950
GPV366
Q132
C)
Y953
Y950
GPV005,
GPV031
Q132R
D)
Y953
Y950
GPV366
Q132R

Molecular Pharmacology

Supplemental Material

Pore exposed tyrosine residues of P-glycoprotein are important hydrogen bonding partners for drugs

Yaprak Dönmez Cakil, Narakorn Khunweeraphong, Zahida Parveen, Diethart Schmid, Matthias Artaker, Gerhard F. Ecker, Harald H. Sitte, Oliver Pusch, Thomas Stockner, Peter Chiba

Supplementary Figure 1

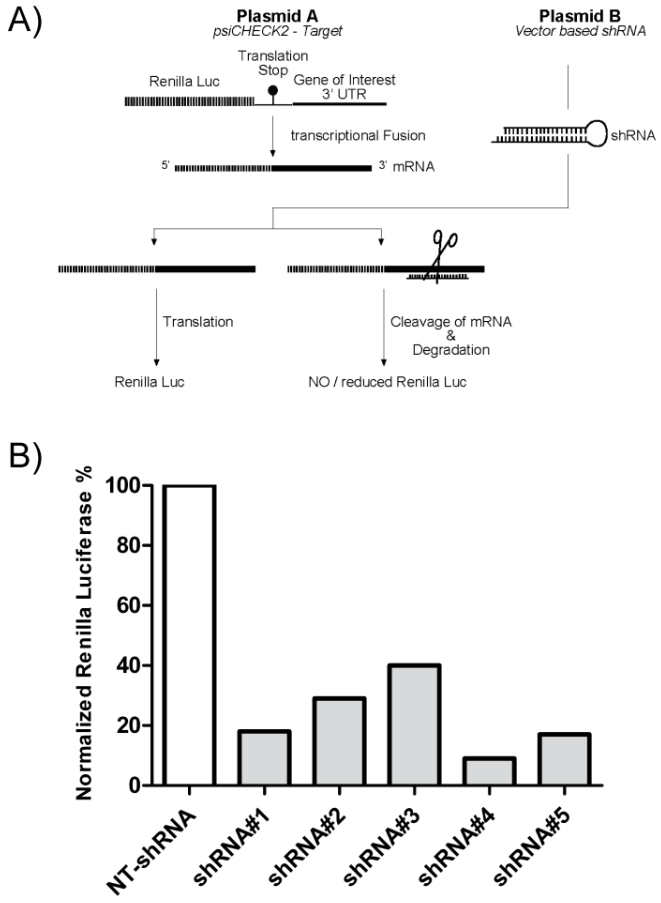

A. Mechanism of action of the siCHECK-2 Vector Reporter System. Plasmid A: The target region (3'UTR of endogenously expressed P-gp) is cloned into the multiple cloning region located 3' to the synthetic Renilla gene and its translational stop codon. Plasmid B: Vector producing short hairpin (sh) RNA. Reporter (Plasmid A) and vector based shRNA constructs

(Plasmid B) are co-transfected into HEK293 cells. A fusion of the Renilla gene and the gene of interest is transcribed. Effective shRNA constructs will initiate the RNAi process towards the target gene. The fused Renilla-gene of interest mRNA will be cleaved and subsequently degraded, decreasing the Renilla luciferase signal.

B. Identification of effective siRNAs targeting the 3 'UTR of endogenous expressed P-gp. A 384 bp fragment corresponding to the 3' UTR region was cloned into the psiCheck 2 Vector, using the Xho I and Not I restriction sites located 3' to the Renilla translational stop codon. Five constructs (#1 - #5) expressing the potential shRNAs were co-transfected into HEK293 cells and analyzed for target mRNA degradation. NT-shRNA is a control vector containing scrambled shRNA (Addgene plasmid # 1864). Constructs #1 and #4 showed most potent target downregulation. Renilla and Firefly luciferase activities were measured 48 hours post transfection using the Dual-Glo Luciferase Assay System (Promega). Renilla luciferase has been normalized to firefly luciferase. Values represent the average of triplicate independent experiments, with the ranges indicated. All shRNA expression cassettes were sequence verified.

Supplementary Figure 2

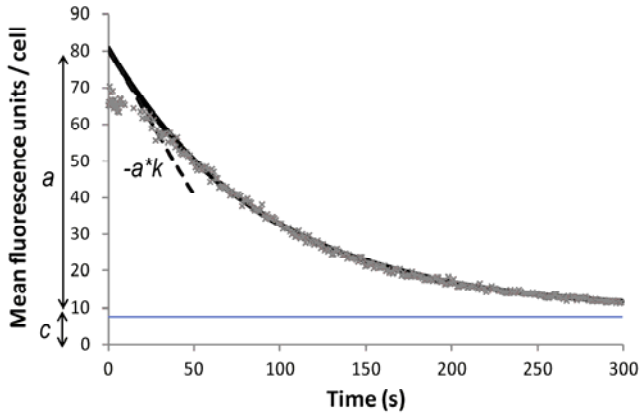

Rh123 efflux was measured continuously over five minutes and mean fluorescence units per cell were determined from about 3000 gated events every second. An exponential curve was fitted to 300 individual data points (x), each representing the average over one second. During the first 30 seconds (resuspension of cells in warm efflux medium) the transport rate is lower, because cells have to readapt from being shifted from ice to 37°C. These data points were therefore excluded from the fit. First order rate constants (*k*-values) were calculated from an exponential fit (solid line) according to the equation $y=a*e^{-kt}+c$, where *a* is the difference between zero and infinite time point of the curve, *e* is the Euler number, *k* is the first order rate constant, *t* is the time in seconds and *c* is the background fluorescence of cells. The slope of the tangent in the origin (stippled line) is *-a*k*. It is important to note that the variable k is thus independent of initial loading, because *-a*k/a* is equal to *-k*. Therefore *-k* can be viewed as a tangent in the origin of the curve for data points referring to fractional cellular fluorescence (normalized initial efflux rate). There is no need for attempting to load cells equally by e.g. depleting them of ATP or inhibiting efflux transport during loading. Both re-establishing cellular energy metabolism after ATP depletion or washing out inhibitors before functional assays could potentially compromise results because of the required time scales.

Supplementary Figure 3

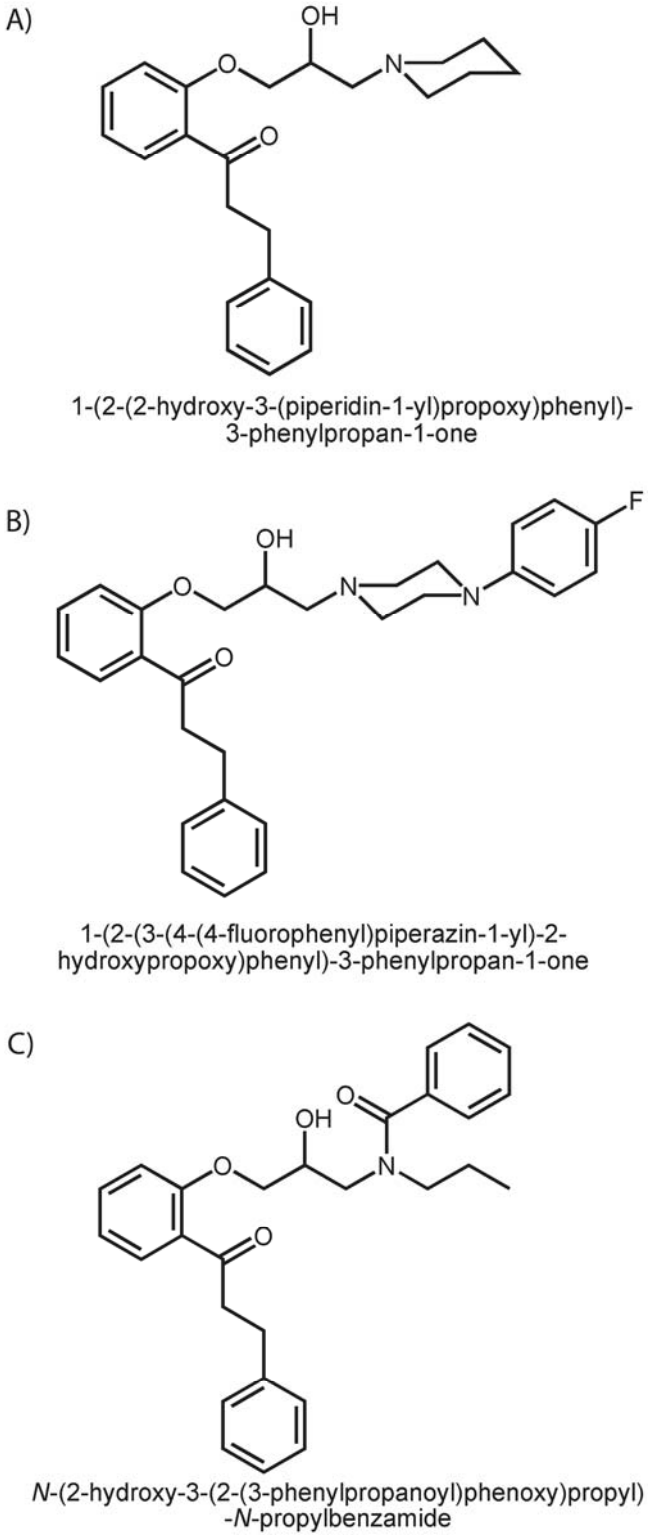

Chemical structures of protonatable propafenones GPV005 **(A)**, GPV031 **(B)** and the non-protonatable acid amide GPV366 **(C)**.

Supplementary Figure 4

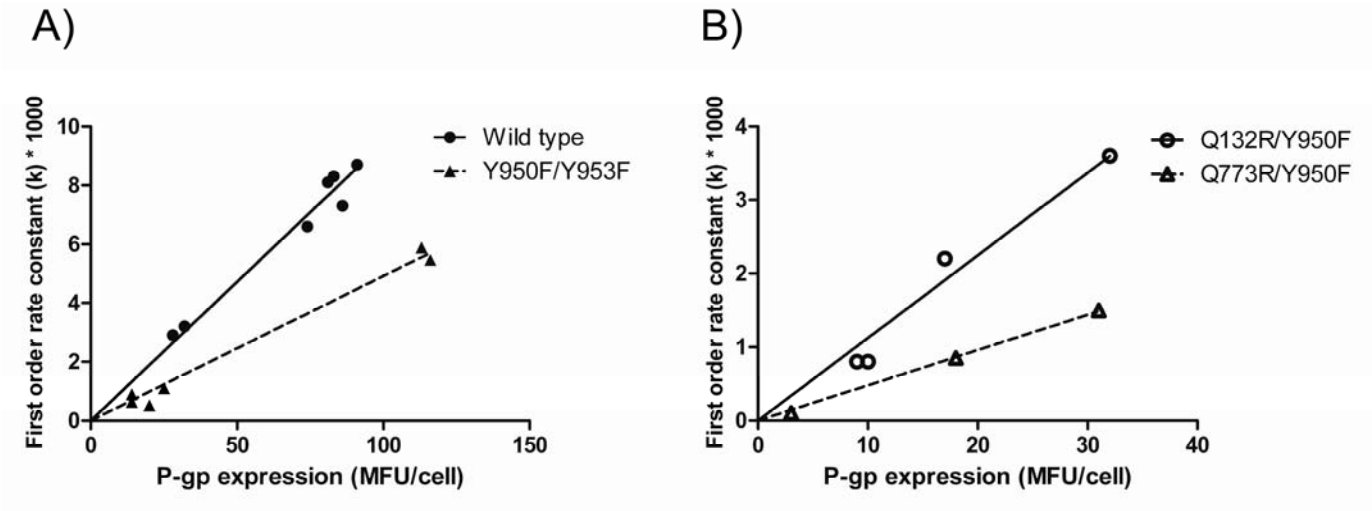

First order rate constants are plotted as a function of P-gp expression in order to show the linear relationship between first order rate constants and expression. Transport measurements were done in duplicates and expression measurements were done in triplicates for each experiment. Mean values are shown for wild type P-gp and the Y950F/Y953F mutant **(A)** and the Q132R/Y950F and Q773R/Y950F mutants **(B)**. The latter show lower surface expression.

Supplementary Figure 5

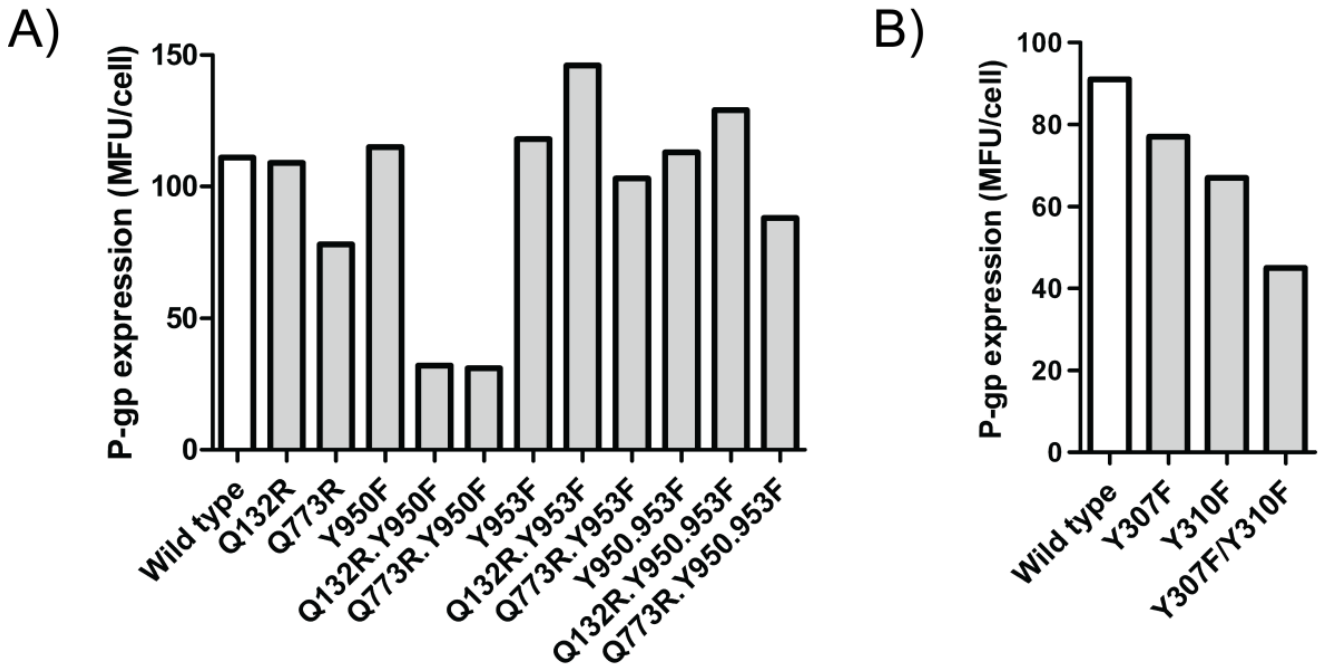

Expression levels of wild type P-gp and tyrosine mutations located in helix 11 **(A)** and helix 5 **(B)**. Data are shown for one representative experiment performed in triplicates. P-gp specific MRK16 antibody was used to determine expression levels and IgG2A was used as the control antibody to correct for non-specific binding.

Supplementary Figure 6

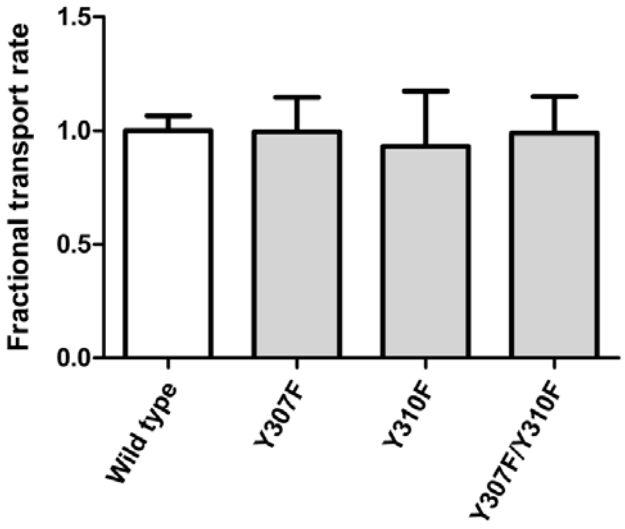

Bar graph showing fractional transport rates of Y307F, Y310F and Y307F/Y310F mutants in comparison with wild type P-gp. First order rate constants (k) for rh123 efflux were calculated from an exponential fit and normalized to surface expression determined by MRK16 staining. Each value represents the mean ± SD of at least 3 independent experiments. No significant difference in transport rates was found in mutants as compared with wild type P-gp.

Supplementary Table 1

	IC_{50} ± SD (nM)		
	GPV005	**GPV031**	**GPV366**
Wild type	518 ± 141	85 ± 22	2239 ±391
Y950F	1348 ± 229	238 ± 84	2984 ± 79
Y953F	1207 ± 362	287 ± 109	15946 ± 2941
Y950F/Y953F	2418 ± 194	630 ± 87	17819 ± 2106
Q132R	1414 ± 215	521 ± 183	1074 ± 282
Q132R/Y950F	1360 ± 387	363 ± 127	966 ± 259
Q132R/Y953F	2164 ± 252	1100 ± 118	3261 ± 965
Q132R/Y950F/Y953F	3367 ± 662	1414 ± 324	5286 ± 1465

IC_{50} values of compounds in wild type and mutants, calculated from concentration response curves by non-linear regression analysis. Each value represents the mean ± SD of at least 3 independent experiments.

Supplementary Table 2
A)

	Significance		
	GPV005	**GPV031**	**GPV366**
Wild type vs. Y950F	***	*	ns
Wild type vs. Y953F	**	**	***
Wild type vs. Y950F/Y953F	***	***	***
Y950F vs. Y953F	ns	ns	***
Y950F vs. Y950F/Y953F	***	***	***
Y953F vs. Y950F/Y953F	***	***	ns

B)

	Significance		
	GPV005	**GPV031**	**GPV366**
Q132R vs. Q132R/Y950F	ns	ns	ns
Q132R vs. Q132R/Y953F	ns	**	*
Q132R vs. Q132R/Y950F/Y953F	***	***	***
Q132R/Y950F vs. Q132R/Y953F	*	***	*
Q132R/Y950F vs. Q132R/Y950F/Y953F	***	***	***
Q132R/Y953F vs. Q132R/Y950F/Y953F	**	ns	*

Statistical significance of differences in IC_{50} values for compounds GPV005, GPV031 and GPV366 in wild type **(A)** and Q132R background **(B)**. *p< 0.05, **p< 0.01 ***p< 0.001